Development of a Low Current Heaterless Hollow Cathode for Hall Thrusters

IEPC-2015-163／ISTS-2015-b-163

*Presented at Joint Conference of 30th International Symposium on Space Technology and Science
34th International Electric Propulsion Conference and 6th Nano-satellite Symposium,
Hyogo-Kobe, Japan
July 4 – 10, 2015*

Dan Lev[1], Gal Alon[2], Dmytry Mikitchuk[3] and Leonid Appel[4]
Rafael - Advanced Defense Systems Ltd., Haifa, 3102102, Israel

Development of low current heaterless hollow cathode at Rafael is presented. The development process encircles cathode design, fabrication and experimentation activities aiming at nominal discharge current operation in the 0.1 A to 1 A range. Initially, manufacturing processes were developed to allow for the use of a variety of materials and geometries for optimal cathode thermal design. Subsequently, commercially available thermal simulation software was utilized to evaluate the temperatures formed on the electron emitter and cathode body. These temperatures were verified by experimentation, therefore validating the thermal model and corresponding assumptions. Cathode end-of-life was reached, as predicted by the thermal model, during operation at discharge current levels above 0.8 A due to excessive emitter heating. The end-of-life failure mechanism was analyzed and verified by comparing the observed phenomenon to literature. The described development campaign provides Rafael with heaterless hollow cathode development capabilities.

Nomenclature

A	=	Surface area
e	=	Electron charge
I_{dis}	=	Discharge current
k	=	Boltzmann constant
m_i	=	Ion mass
m_e	=	Electron mass
$\dot{m}$	=	Cathode mass flow rate
n_e	=	Plasma density
P_{tot}	=	Total power
P_{i}	=	Ion flux power deposition
P_{e}	=	Electron flux power deposition
R_{pl}	=	Plasma channel resistance
T_{eV}	=	Electron temperature
U^+	=	Ionization potential
$\varphi_{s,o}$	=	Orifice sheath potential drop
$\varphi_{s,e}$	=	Emitter sheath potential drop
φ_{wf}	=	Emitter work function
$\Delta\varphi_{e\text{-}o}$	=	Emitter-orifice potential difference
$\Delta\varphi_{res}$	=	Plasma channel potential drop

[1] Ph.D., Electric Propulsion R&D Responsible, Rafael, Manor Division, Space Department, danle@rafael.co.il.
[2] Mechanical Research Engineer, Rafael, Manor Division, Space Department, galalo@rafael.co.il.
[3] Plasma Research Physicist, Rafael, RDE Division, dmytrym@rafael.co.il.
[4] Mechanical Research Engineer, Rafael, Manor Division, Space Department, leona@rafael.co.il.

I. Introduction

HEATERLESS Hollow Cathodes (HHCs) are a subclass of hollow cathodes that do not require external heating to heat up the electron emitter to its operation temperature. Instead of using external heating HHCs use a unique ignition technique. Firstly, high voltage pulse is applied between the emitter and keeper so to breakdown the injected gas. Immediately after the initial discharge creation a separate power supply controls the emitter-keeper current, a process during which the emitter is heated via ion bombardement. The heating process lasts until the emitter reaches its operation temperature and the voltage drops to a few tens of volts. Lastly, after steady discharge has been initiated the electric thruster is turned on by applying the required emitter-anode current. The entire thruster ignition duration is less than ten seconds.

Since HHCs do not use external heating for ignition they posses advantages over their heater-utilizing cousins. First, In comparison to heater-utilizing cathodes that have typical readiness time in the order of minutes, due to the required heating duration, HHCs reach steady-state operation within seconds. Secondly, since no external heating is required the Power Processing Unit (PPU) does not contain the corresponding heater module, therefore lowering its mass. Lastly, since the discharge in HHCs is self sustaining these cathodes are energy efficient relative to heater-utilizing cathodes[1].

Heaterless hollow cathodes have been explored in the past and shown to operate adequately both against a simple plate, serving as the anode[2,3], or coupled with Hall thrusters[1,4,5]. This type of hollow cathode is under investigation and development around the world thanks to the advantages these cathodes posses. Nevertheless, HHCs have a disadvantage when delivering low current in the order of ~0.1-1 A since no additional external heating can be applied to compensate for the lack of heating from the low discharge current. For this reason HHCs designed to deliver low current must have thermally-efficient structure to maintain the required emitter temperatures during emitter-anode steady-state operation. In addition, because thermally-efficient design naturally contains refractory metals it is essential to develop manufacturing processes that allow for proper leak-tight connectivity of the cathode parts.

In recent years Rafael has been investigating low current HHC physics for igniting and neutralizing low power Hall effect thrusters[2,6]. Particular attention and efforts are invested in (a) Thermally-efficient design (b) development of manufacturing processes and (c) ability to operate with various commercially available emitters.

The purpose of the research described in this paper is to validate design and manufacture capabilities of HHCs. Proper thermal design was done through an adequate choice of materials and cathode geometry. In parallel with the design phase development of suitable manufacture processes was conducted so to allow for the realization of the selected thermal design.

This paper describes the thermal analysis performed on a laboratory model of Rafael's Heaterless Hollow Cathode (RHHC) followed by validation experiments. The heaterless hollow cathode is presented in Figure 1. The experimental validation phase concluded with current limit determination that was achieved by gradual increase of cathode current until intentional thermal and mechanical failures occurred. The paper concludes with conclusions and future work.

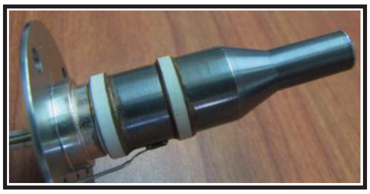

Figure 1. Picture of Rafael's Hollow Heaterless Cathode (RHHC)

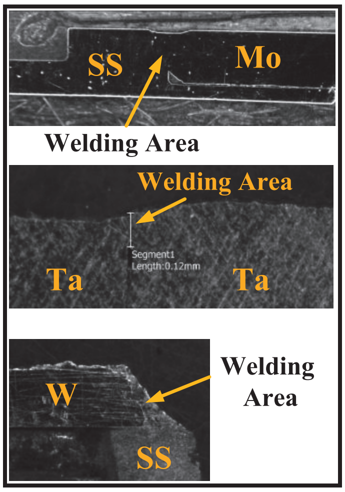

Figure 2. Pictures of metalographic welding samples

II. Cathode Description

Rafael's Heaterless Hollow Cathode (RHHC) is a laboratory cathode manufactured in order to validate thermal design capabilities and develop manufacturing processes. Prior to the structure design process it was indicated that the major challenge in low current hollow cathode design is a suitable thermal design dedicated to maintaining the required operating temperatures of the electron emitter. To do so several guide lines and actions were followed: (a) an impregnated tungsten (W-BaO) low work function emitter was chosen, (b) low thermal conductivity refractory metals were used and (c) high aspect ratio geometries were chosen.

Two commercially available barium oxide impregnated tungsten emitters were chosen, each with a different internal diameter. These emitters have a known work function of approximately 2 eV and have been used extensively in the past in electric propulsion applications[7,8]. The cathode external module, referred to as the keeper module, as well as the internal module, referred to as the emitter module, are mostly composed of known refractory metals - tungsten (W), tantalum (Ta) and molybdenum (Mo). Since Ta has the lowest thermal conductivity it was extensively used as the main structural material in high temperature regions. Machining techniques were developed to fabricate large aspect ratio refractory metal parts with thicknesses as low as 0.35 mm.

Connections between two refractory metal parts as well as refractory metals to stainless steel parts were performed using special welding techniques developed particularly for this purpose. Pictures of metallographic samples are presented in Figure 2. The welding techniques allow for localized heating of metal at the intended welding spot hence avoiding the temperature raising of the entire part, maintaining it below the Ductile to Brittle Transition Temperature (DBTT) and keeping its grain size unchanged. To validate proper mechanical connectivity all welding processes were leak tested and found leak-sealed.

Lastly, to adequately monitor cathode manufacturing and assembly processes the manufacturing design allowed for separate examination and leak test of each cathode module and subassembly, therefore allowing proper quality assurance in the manufacturing and assembly phase.

III. Thermal Model

Since no direct experience in low current cathode thermal design existed in Rafael prior to the design phase the goal of the laboratory model was to gain thermal design capabilities by designing a cathode able to operate at a nominal current of less than 0.5 A. Developing such design capabilities will enable future design campaigns of higher current cathodes.

The thermal design phase included thermal analysis with the purpose of reaching simulated steady state emitter temperatures of around 1000°C which are necessary for sufficient electron emission[9].

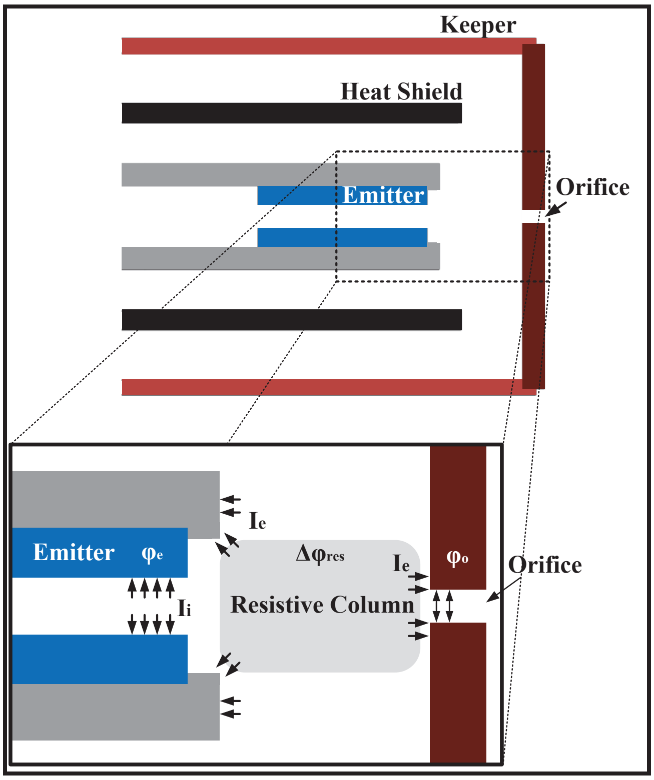

Figure 3. Illustration of the internal structure of the cathode. The zoomed in view presents the modeled emitter-keeper gap.

A. Input Power Estimation

As a preliminary phase the input power to various parts of the cathode had to be determined for different cathode current values. To do so a basic model was formulatted in which the physical mechanisms within the emitter-keeper gap are described (Figure 3). It is assumed that the cathode is at steady state operation, therefore the emitter-keeper electrical circuit is inactive and the keeper is electrically floating. It is assumed that the electron temperature is constant at 1 eV throughout the emitter-keeper gap. This value of electron temperature is characteristic in hollow cathodes[7] thus valid for the purposes of this model. It is assumed that emitter heating is due to ion flux, accelerated through the cathode sheath, and impinging on the emitter surface.

1. Total Heating Power

Total power to the cathode can be estimated as

$$P_{tot} = I_{dis}\left(\Delta\varphi_{e-o} + \varphi_{s,o}\right), \tag{1}$$

where I_{dis} is the main discharge current, $\Delta\varphi_{e\text{-}o}$ is the emitter-orifice potential difference and $\varphi_{s,o}$ is the orifice sheath potential fall. The emitter-orifice potential difference, $\Delta\varphi_{e\text{-}o}$, is determined from preliminary experiments and was found to be $\Delta\varphi_{e\text{-}o}$=14-10($I_{dis}$-0.4) volts. This measurement is in accord with similar measurements taken by Vekselman on a similar heaterless hollow cathode[2] under similar operating conditions. The orifice sheath potential, $\varphi_{s,o}$, can be estimated by using the assumption that the keeper structure is electrically floating thus $\varphi_{s,o}= T_{eV}\cdot\log(m_i/2\pi m_e)^{1/2}$, where T_{eV} is the electron temperature in units of eV (1 eV).

2. Emitter Heating Power

It is postulated that the ion flux is generated by full and single ionization of the xenon atoms passing through the emitter tube. The nominal cathode mass flow rate was determined as 0.15 mg/s by similarity to other low current hollow cathodes[4,5,10,11]. Therefore the impinging ion current is $I_i=(e/m_i)\dot{m}$ where e is the elementary electron charge, m_i is the xenon ion mass and $\dot{m}$ is the cathode mass flow rate. The ion heating to the emitter is

$$P_i = I_i\left(U^+ + \varphi_{s,e} + T_{eV}/2 - \varphi_{wf}\right), \tag{2}$$

where U^+ is xenon's ionization potential (12.1 eV), $\varphi_{s,e}$ is the cathode emitter sheath potential and φ_{wf} is the emitter material work function (2 eV). Cathode emitter sheath potential is calculated from the potential balance within the emitter-keeper gap

$$\varphi_{s,e} = \Delta\varphi_{e-o} + \varphi_{s,o} - \Delta\varphi_{res}, \tag{3}$$

where $\Delta\varphi_{res}$ is the voltage fall due to plasma channel resistance. $\Delta\varphi_{res}$ was estimated by Vekselman[2] for a similar heaterless cathode under the same assumptions as $\Delta\varphi_{res}=I_{dis}R_{pl}$, where and R_{pl} is the plasma channel resistance calculated as 14 Ω.

Electron heating to the emitter, that scales with $\exp(\varphi_{s,e}/T_{eV})$, is neglected due to the relatively high cathode sheath potential, in the order of ~10 V driving the value of the random electron flux to very low values.

3. Emitter tube and orifice Heating Power

The heating power that is not inflicted on the emitter is dissipated into the mechanical components adjacent to the plasma discharge, namely the orifice plate and the structure supporting the emitter, the emitter tube. In these regions it is assumed that heating is mainly due to random electron current impinging on the mechanical surfaces. The random electron current can be estimated by[7]

$$P_e = \left(2T_{eV} + \varphi_{wf}\right)\frac{1}{4}\left(\frac{8kT_e}{\pi m_e}\right)^{1/2} n_e e A \exp\left(-\frac{\varphi_s}{T_{eV}}\right), \tag{4}$$

where k is Boltzmann constant, m_e is the electron mass, n_e is the bulk plasma density, A is the surface upon which the electrons are impinging and φ_s is the local sheath potential. Since several parameters, specifically the number density, are unknown to a reasonable level for the analysis presented here it is assumed that the heating power not invested in direct emitter heating is evenly distributed between the orifice plate and emitter tube, $(P_{tot}-P_i)/2$. This assumption is acceptable in light of the fact that the main emitter heating mechanism is due to direct ion impingement on the emitter surface.

Using the relations and assumptions stated above we arrive at the heating power, dissipated into the emitter surface and supporting tube (emitter module) and orifice plate (keeper module), as a function of the discharge current. The heating power values are presented in Figure 4.

These boundary conditions support the thermal simulation presented in the subsequent subsection.

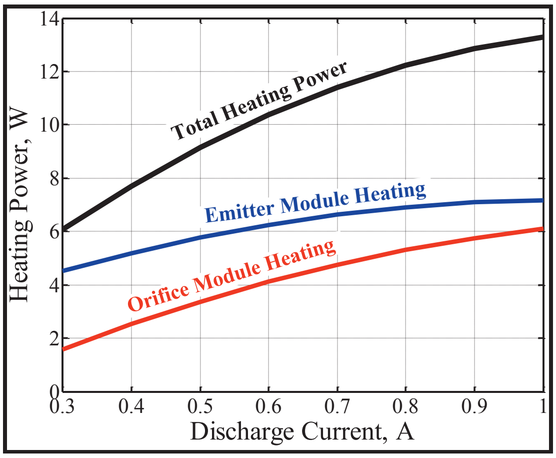

Figure 4. Computed heating power boundary conditions for the thermal simulation

B. Computentional Method, Assumptions and Boundary Conditions

Thermal simulation was performed using the Thermal Analysis Module of 'Solidworks' Simulation 2014 by 'Dassault Systems'. The cathode was meshed to 40,000 tetrahedral elements and P-method convergence demonstrated; therefore the thermal simulation results presented hereafter are satisfactory. Emitter heating power is described in previous sections. The temperature at the cathode base was set to 20°C, while the ambient temperature was set to 25°C for radiation purposes. Due to high vacuum conditions, heat transfer by convection was neglected;

therefore the simulation accounts for heat transfer by conduction and radiation only. Thermal contact resistance was applied between any two interfacing surfaces. The emitter's thermal conductivity was set to 70 W/m·K[12,13], while all other thermal conductivities and emissivities were set according to raw materials' manufacturers and by common engineering datasheets from multiple sources.

C. Thermal Simulation Results

Thermal simulation was performed to obtain an estimate for the emitter temperatures at different cathode operational conditions. As such the simulation was executed for discharge current of 0.3 A, 0.5 A, 0.8 A and 1 A.

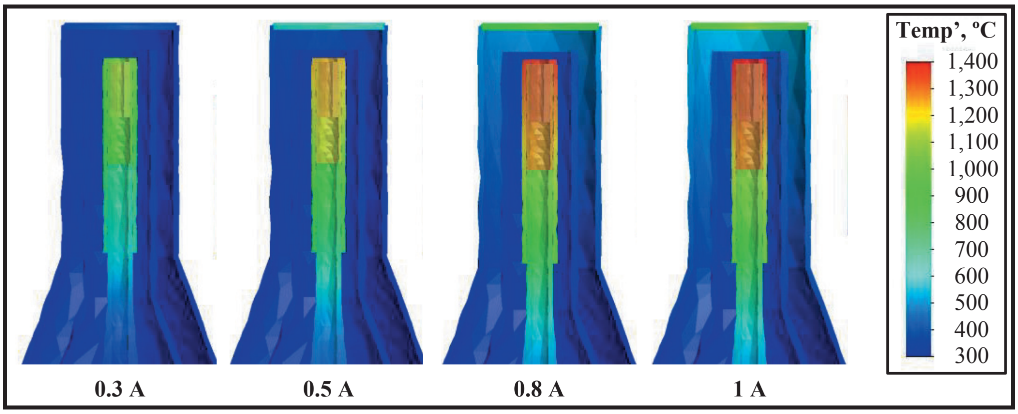

Figure 5. Crossectional view of the thermal simulation results for discharge current of 0.3 A, 0.5 A, 0.8 A and 1 A.

The corresponding results are presented in Figure 5. It can be observed from the figure that the emitter temperature ranges from about 1000°C at discharge current of 0.3 A to over 1300°C at discharge current of 1 A. It can also be observed that the orifice plate temperature is approximately uniform and does not exceed 900°C at the hottest scenario investigated at 1 A. The simulation results indicate that the cathode may operate at discharge current as low as 0.3 A. Addditionally, it can be concluded from the simulation results that excessive emitter heating is expected at discharge current of 0.8 A and higher. This issue is addressed and verified in the experimental phase of the work presented in this paper.

It is interesting to note that the temperature distribution along the emitter is relatively "mild" and extends along ~30 K over a few milimeters. This result implies that during cathode operation most of the emitter surface is at the required emission temperature and can take part in cathode staedy state operation. This result is in accord with previous work on BaO-based hollow cathodes[14].

It should also be noted that the emitter module is experiencing temperature gradients from over 1000°C at the tip, depending on the discharge current, and down to less than 600°C at the emitter module middle section, roughly 25 mm from the tip. These sharp temperature gradients are attributed to the emitter module low thermal conductivity and large aspect ratio with thickness as low as 0.35 mm.

Simulated external body temperatures of the cathode for discharge current of 0.5 A and 0.8 A are presented in Figure 6. It is observed from the figure that the cathode's external body temperatures range from approximatelly 100°C at the cathode root and up to about 400°C at the keeper end, close to the orifice plate. These simulated results are used to validate the thermal model by comparing them to actual temperature measurements in the experimental phase.

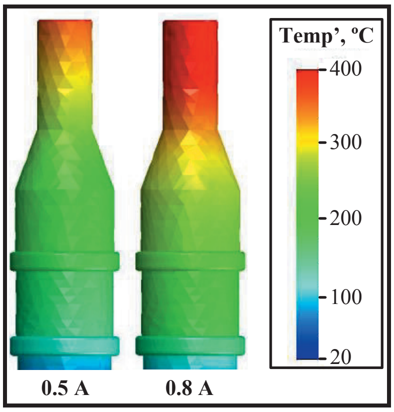

Figure 6. Thermal simulation results of the cathode external body for discharge current of 0.5 A and 0.8 A.

IV. Experimental Validation

A. Test Facility

Development tests were conducted in Cathode Chamber 4 (CC-4), at the Rafael Electric Propulsion Test Facility (Figure 7). CC-4 is a Ø 0.8m × 0.8m stainless steel vacuum chamber with inner volume of approximately 0.4 m^3.

The chamber is equipped with an 'Alcatel-Adixen' model 'ACP28' forevacuum pump with pumping speed of 8 liter/s of air. One 'Austin Scientific' model 'CryoPlex 10' cryopump is located on the bottom flange of the vacuum chamber, isolated by a gate valve. The combined measured pumping speed achieved is approximately 1,000 liter/s of xenon. The residual pressure of the vacuum chamber is lower than 5×10^{-7} Torr. During Cathode operation at a total flow rate of 0.25 mg/s of xenon, chamber pressure was lower than 1×10^{-4} Torr.

Pressure is measured using an 'MKS' cold cathode micro-pirani transducer, model '972B', located behind the anode. The pressure transducer is calibrated by the manufacturer and has a declared precision of 30% in high vacuum. Cathode mass flow is controlled by a 'Tylan' model 'FC2900' flow controller, in the range of 0÷0.5 mg/s with a declared precision of 1% of full scale.

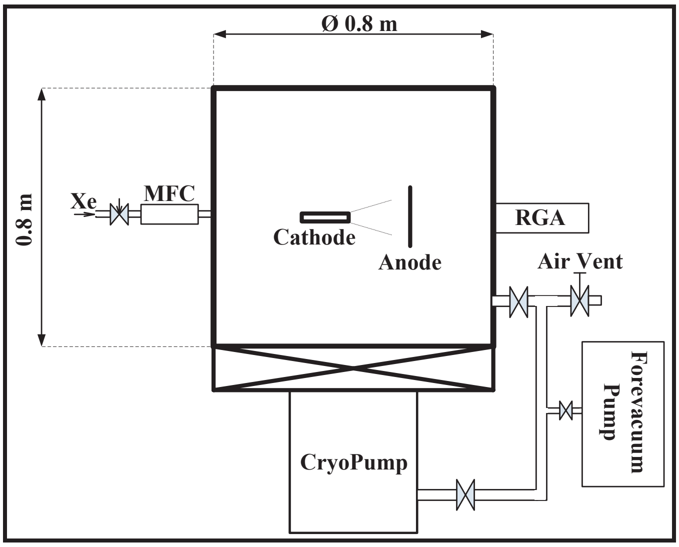

Figure 7. Schematic of the Rafael Cathode Chamber.

B. Experimental Setup

The cathode was mounted on an electrically floating bracket. The cathode was positioned so that the cathode's orifice plate was located 25 mm to 40 mm from the anode, which is electrically floating relative to ground. Schematic of the experiemental setup is presented in Figure 8.

Three ungrounded K-type thermocouples were positioned along the cathode's longitudinal axis and were used to measure temperature during operation (Figure 9). Temperature data acquisition was performed using 'Fluke' model '287' digital multimeter.

The electrical setup consisted of a 'TDK-Lambda' model 'GEN600-4' power supply used for the main anode discharge and an in-house cathode startup power supply used for cathode ignition (Figure 10). The startup power supply was fed by a 'Stanford Scientific' High Voltage (HV) power supply and a 'TDK-Lambda' model 'GEN300-5' power supply. The HV power supply provided the required plasma breakdown voltage while the keeper power supply provided the power necessary to sustain the discharge prior to cathode-anode circuit activation. The startup power supply is responsible for properly sequensing, modifying and regulating the input signal to the cathode keeper. A 100 Ω ballast resistor was connected on the cathode-anode line to limit possible high current "spikes" during ignition and protect the anode discharge power supply.

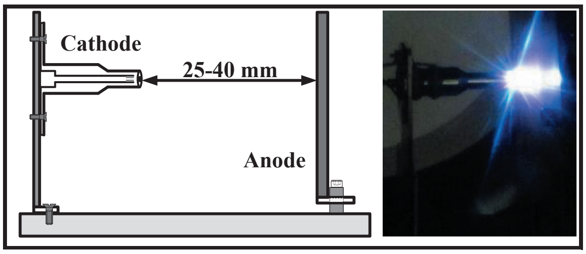

Figure 8. Left: Schematic of the experimental setup, Right: Picture of the experimental setup during cathode operation.

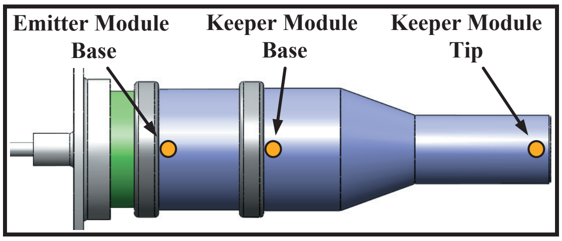

Figure 9. Thermocouple positioning along the cathode body.

C. Test Plan

The purpose of the test plan was to validate the thermal model by (a) external cathode body temperature measurement and (b) identyfing the cathode's current upper limit and correlating it to expected behavior at excessive emitter temperatures as found in the thermal

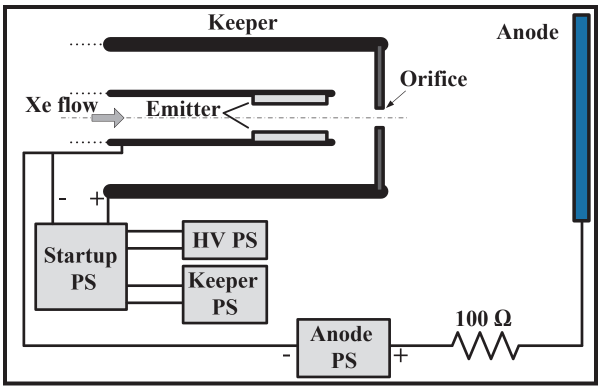

Figure 10. Electrical scheme of the cathode experimental setup.

model.

The test plan included cathode-anode steady state operation at current levels from 0.2 A to 1 A, with increments of 0.1 A, at cathode mass flow rate of 0.15 mg/s. Discharge current increase was gradual and monotonically ascending with varying operation duration at each current level. The cathode was operated at least 30 minutes at each discharge current level and temperature measurement taken at the end of each session.

Particular attention was given to current levels of 0.3 A, 0.5 A, 0.8 A and 1 A where the cathode was operated for several hours during which cathode-anode voltage characteristics were collected as well as cathode body temperature measurements. During high current operation above 0.7 A occasional lower current operations were attempted to monitor any change in the cathode's characteristics at lower current levels.

All cathode startup sequences were conducted by a preliminary emitter-keeper stratup sequence in order to initiate cathode discharge. No longer than five seconds after cathode discharge was initiated the main anode discharge power supply was turned on simultaneously with the startup power supply shut down.

D. Results

Cathode operation went as planned with ignition breakdown voltages of less than 1000 V for most cases investigated. For all operations a clear and steady ball-like discharge was spotted near the cathode orifice thus indicating spot-mode operation. Anode voltages were steady to within 2% of measured voltage, repeatable to within 30 minutes of initial measurement and increasing by about 25% throughout the entire experiment. Speculation for the cause of the gradual change in discharge voltage is presented in the following section.

Cathode operation was successful, yet unsteady, at discharge current of 0.2 A. At this current level sporadic discharge extinguishing was experienced. Nevertheless, at current levels of 0.3 A and above the cathode exhibited steady and self-sustainable operation.

1. Temperature Measurements

For each of the discharge current level explored the measured temperatures from each one of the thermocouples increased after the cathode was operated at higher discharge current levels. For example, initial keeper module base temperature at 0.5 A was measured under 200°C in steady state. Subsequently, throughout the experimental campaign and after at least 10 hours of operation at current levels higher than 0.8 A the measured temperature at 0.5 A went up by more than 20°C. This behavior was observed for all current levels and was accompanied by ignition difficulties near the end of the experimental campaign. Measured cathode temperatures as well as simulated temperatures at the thermocouple positions are presented in Table 1 for comparison.

Table 1. Simulated and measured cathode body temperatures for discharge current of 0.5 A and 0.8 A. Measured accuracy is deduced from the constant increase in measured temperature as a consequence of the gradual heating of the emitter.

Position	Discharge Current			
	0.5 A		0.8 A	
	Simulation	Measurement	Simulation	Measurement
Emitter Module Base	*170°C*	*200±35°C*	*200°C*	*230±30°C*
Keeper Module Base	*200°C*	*200±15°C*	*250°C*	*245±10°C*
Keeper Module Tip	*320°C*	*260±40°C*	*360°C*	*315±30°C*

It can be seen in the table that emitter module base and keeper module base temperatures were well predicted and within the measuring range that was estimated from the slow increase in measured temperatures. This matching between the thermal simulation and actual measurements streightens the assumptions taken while forming the simulation. At the same time there are discrepancies between keeper module tip simulated and measured temperatures. The discrepancies can be attributed to inadequate contact between the thermocouple and keeper body due to high keeper curvature at the measured location or mispositioning because of limited access and maneuverability in the vacuum chamber. It can be concluded that to a sufficient extent the thermal simulation predicts cathode thermal behavior at varying discharge current levels.

2. Cathode End-of-Life Analysis

After several hours of operation at current above 0.7 A cathode operation became impossible at discharge current levels of 0.3 A. Additional cathode operation at current levels above 0.8 A led to cathode startup difficulties and spontanious operation halt at lower current. Finally, after several hours of cathode operation at 1 A the cathode line became "clogged", with no xenon passing through. At this point further cathode operation was impossible and it was decided to conclude the experiment.

The thermal simulation predicts temperatures above 1300°C at the high end of the explored current level range. This temperature range for W-BaO based emitters is excessive, expected to cause rapid emitter degradation and eventually lead to cathode failure[15-19]. Consequently, the cathode destruction mechanism was investigated by dissecting the cathode and using micro-images, SEM and X-ray diagnostics to analize the post-test emitter.

It was found that the inner emitter tube diameter essentially reduced to zero (Figure 11). The materials covering the tube hole were molybdenum (Mo) and tantalum (Ta) which are the materials encapsulating the emitter and emitter tube. Furthermore, the coverage structure points at molybdenum and tantalum melting which is expected at elevated temperatures of over 2600°C. Essentially the emitter tube looked as if its interior melted and mixed with the exterior sections. Additionally, little to no traces of Ba were found on the emitter surface; therefore indicating that either barium oxide deplition occurred or that the emitter surface was covered with molten metal.

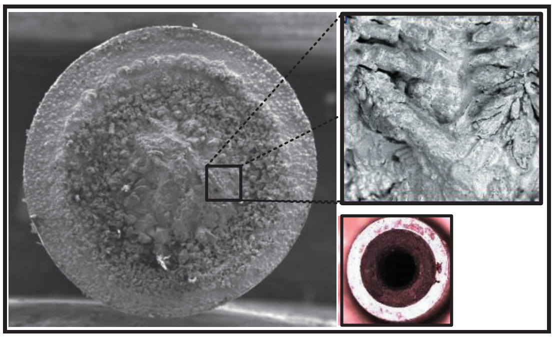

Figure 11. Left: Micrograph of the "plugged" emitter tube after cathode end-of-life. Top-Right: Image enlargement showing Mo melting traces. Bottom-Right: micrograph of a fresh unused emitter.

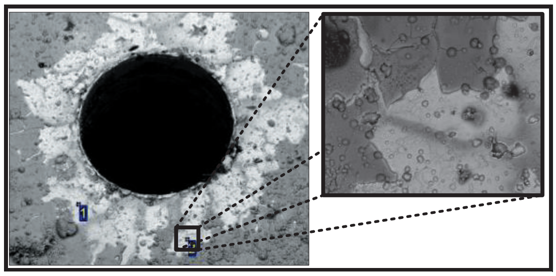

Figure 12. Left: Micrograph of the inner side of the cathode orifice after cathode end-of-life. Top-Right: Image enlargement showing tungsten sputtering traces around the orifice.

Further analysis performed on the inner side of the keeper orifice showed clear Tungsten (W) sputtering marks, which should be found only in the emitter matrix (Figure 12). In addition to tungsten traces of barium and oxygen were also found around the orifice. The traces indicate that oxidized tungsten formed in the emitter-keeper gap and migrated to the orifice, most likely through upstream incoming xenon pressure from the emitter tube.

E. Discussion

The processes occuring inside the cathode during its operation are in accord with existing hollow cathode knowledge and simulated emitter temperature. The ability to ignite the cathode at discharge current levels of 0.3 A corresponds to the results obtained from the thermal simulation. In the same manner, difficulties in maintaining steady cathode operation at 0.2 A were expected since simulation results indicate emitter temperatures lower than 1000°C that are not sufficient for forming sustainable discharge[9,17,18].

It is postulated that cathode operation at current levels of 0.5 A or lower is suitable for the designed cathode with expected emitter temperatures of 1000°C to 1200°C. However, at higher discharge current operation expected emitter temperatures are higher, leading to accelerated barium oxide depletion[9,15,17,18]. As barium oxide vaporized from the emitter surface and depleted the effective emitter work function increased. The increase in work function leads to an increase in cathode sheath potential since the ions require greater energy to impact the emitter and increase its temperature further so it emits the required electron flux to maintain the discharge. This behavior was observed indirectly by the gradual rise in the required cathode-anode voltage at the examined discharge current levels. The rise in discharge voltage was accompanied by an increase in exeterior cathode body temperature which is an indication for emitter temperature rising. As emitter temperatures rise the process worsens by faster barium oxide depletion, additional increase in work function and higher power deposited into the emitter. During the described process cathode temperatures may reach temperatures of well over 2500°C and cause structural meltdown or vaporization. Eventually cathode operation is impaired to the point of failure as was previously observed in literature[19].

In the future the above-described phenomena can be avoided by either operating the cathode at the allowed discharge current levels or by designing it to the required operational point in term of discharge current.

V. Conclusion

This paper presents the development campaign of a low current heaterless hollow cathode which was designed, fabricated and operated by Rafael. As part of the described endeavor speacial manufacturing processes were developed to allow for the use of a variety of materials and geometries for optimal cathode thermal design. Subsequently, commercially available thermal simulation software was used to compute and evaluate the temperatures formed on the emitter surface and cathode body. The thermal model was validated by experimentation during which the cathode was operated in diode mode at discharge current levels of 0.3 A to 1 A. Thermal model validation was conducted by measured cathode body temperatures that were in acceptable agreement with the simulated results. Finally, cathode end-of-life was reached by an operation at the high end of the discharge current levels explored and were equivalent to the expected emitter destruction temperatures computed by the thermal simulation. Cathode end-of-life was associated with elevated emitter temperatures, barium oxide depletion and eventually inner emitter tube plug. Postulation of the physical processes leading to the phenomena described is raised and based on existing literature.

Rafael now possesses the required tools for proper heaterless hollow cathode design and manufacture. Future research will focus on ignition process optimization and higher operational current designs.

References

[1]R. Albertoni, M. Andrenucci, D. Pedrini and F. Paganucci. "Preliminary Characterization of a LaB6 Hollow Cathode for Low-Power Hall Effect Thrusters". *Proceedings of the 33rd International Electric Propulsion Conference (IEPC)*, 6-17 October, 2013, Washington D.C., USA, IEPC-2013-137.

[2]Vekselman, V., Krasik, Ya. E., Gleizer, S., Gurovich, V. Tz., Warshavsky, A. and Rabinovich, L., "Characterization of a Heaterless Hollow Cathode," *Journal of Propulsion and Power*, Vol. 29, No. 2, pp. 475-486, 2013.

[3]B. Rubin and J. D. Williams. "Hollow Cathode Conditioning and Discharge Initiation Studies". Colorado State University, Fort Collins, CO, USA. *Technical Paper*, 2007.

[4]A. Loyan, M. Titov, O. Rybalov and T. Maksymenko. "Middle power Hall Effect Thrusters with centrally located cathode". *Proceedings of the 33rd International Electric Propulsion Conference (IEPC)*, 6-17 October, 2013, Washington D.C., USA, IEPC-2013-410.

[5]N. N. Koshelev and A. Loyan. "Investigation of Hollow Cathode for Low Power Hall Effect Thruster," *Proceedings of the 30th International Electric Propulsion Conference (IEPC)*, 17-20 September, 2007, Florence, Italy, IEPC-2007-103.

[6]V. Vekselman, D. Levko, Ya. E. Krasik and I. Haber. "A Comparative Study of Heaterless Hollow Cathode: 2D PIC Modeling vs. Experimentation". *Proceedings of the 33rd International Electric Propulsion Conference (IEPC)*, 6-17 October, 2013, Washington D.C., USA, IEPC-2013-380.

[7]Dan M. Goebel & Ira Katz. Fundamentals of Electric Propulsion: Ion and Hall Thrusters. JPL Space Science and Technology Series, Jet Propulsion Laboratory & California Institute of Technology, 2006.

[8]Dennis L. Tilley, Gary F. Willmes, Roger M. Myers and Richard D. Smith. "Flight Hollow Cathode for Hall Thruster Applications". *Proceedings of the 34th Joint Propulsion Conference (JPC),* 12-15 July, 1998, AIAA-98-3339.

[9]J. L. Cronin. "Modern Dispencer Cathodes," *IEE Proc.,* Vol.128, Pt. I, No. 1, February 1981.

[10]Matthew T. Domonkos, Alec D. Gallimore, George J. Williams Jr. and Michael J. Patterson. "Low-Current Hollow Cathode Evaluation". *Proceedings of the 35th Joint Propulsion Conference (JPC),* June, 1999, Los Angeles, CA, USA, AIAA-99-2575.

[11]Matthew T. Domonkos, Alec D. Gallimore and Michael J. Patterson. "An Evaluation of Hollow Cathode Scaling to Very Low Power and Flow Rate," *Proceedings of the 25th International Electric Propulsion Conference (IEPC)*, 24-28 August, 1997, Cleaveland, OH, USA, IEPC-97-189.

[12]P. I. Mal'ko, V. F. Nemchenko and S. N. L'vov, "Calculation of the Thermal and Electrical Conductivities of Porous Tungsten by Means of Unified Conduction Formulas," *Poroshkovaya Metallurgiya*, Vol. 67, No. 7, pp. 55-59, 1968.

[13]A. V. Pustogarov, G. N. Mel'nikov, A. N. Kolesnichenko, V. D. Daragan and D. D. Chepiga, "Thermophysical Properties of Porous Tungsten at Temperatures of 1200-3200K," *Poroshkovaya Metallurgiya*, Vol. 143, No.11, pp. 52-57, 1974.

[14]James Polk, Colleen Marrese, Ben Thornber, Lisa Dang and Lee Johnson. "Temperature Distributions in Hollow Cathode Emitters," *Proceedings of the 40th Joint Propulsion Conference (JPC),* 11-14 July, 2004, Fort Lauderdale, FL, USA, AIAA-2004-4116.

[15]James E. Polk, Ioannis G. Mikellides, Angela M. Capece and Ira Katz. "Barium Depletion in Hollow Cathode Emitters". *Proceedings of the 45th Joint Propulsion Conference (JPC),* 2-5 August, 2009, Denver, CO, USA, AIAA-2009-5197.

[16]James Polk, Ioannis G. Mikellides, Ira Katz and Angela M. Capece. "Tungsten and Barium Transport in the Internal Plasma of Hollow Cathodes," *Proceedings of the 44th Joint Propulsion Conference (JPC),* 21-23 July, 2008, Hartford, CT, USA, AIAA-2008-5295.

[17]E. S. Rittner, W. C Rutledge and R. H. Ahlert, "On the Mechanism of Operation of the Barium Aluminate Impregnated Cathode," *Journal of Applied Physics*, Vol. 28, No. 12, pp. 1468-1473, 1957.

[18]Michele Coletti and Stephan B. Gabriel, "Barium Oxide Depletion from Hollow-Cathode Inserts: Modeling and Comparison with Experiments," *Journal of Propulsion and Power*, Vol. 26, No. 2, pp. 364-369, 2010.

[19]Sarver-Verhey, T. R., "Destructive Evaluation of a Xenon Hollow Cathode after a 28,000 Hour Life Test," NASA/CR-1998-208678